# Channel Prediction aided Coded Modulation assisted Eigen Beamforming

S. X. Ng, W. Liu, L.-L. Yang and L. Hanzo
School of ECS, University of Southampton, SO17 1BJ, United Kingdom.
Tel: +44-23-8059 3125, Fax: +44-23-8059 4508
Email: {sxn,wl03r,lly,lh}@ecs.soton.ac.uk, http://www-mobile.ecs.soton.ac.uk

***Abstract*— Eigen beamforming is capable of providing useful beamforming gain in a Multiple-Input Multiple-Output (MIMO) system when perfect Channel State Information (CSI) is available. However, when a realistic channel preditor is used to predict the CSI, a significant performance degradation would incur due to phase ambiguity inherent in the estimated eigen-vectors. In this contribution, Coded Modulation (CM) schemes and Differential CM schemes are employed for assisting the eigen-beamforming system when employing a minimum mean square error based channel predictor. It is shown that Differential CM schemes are capable of assisting the beamforming MIMO system for attaining a coding gain of about 6.5 dBs when communicating over correlated Rayleigh fading channels.**

## I. Introduction

A transceiver employing multiple transmitters and multiple receivers is among the most efficient techniques designed for providing high data rates by exploiting the high channel capacity potential of Multiple-Input Multiple-Output (MIMO) channels [1], [2]. On one hand, Space-Time Coding schemes [3], [4] are capable of attaining spatial diversity gains without needing Channel State Information (CSI) at the transmitter. On the other hand, transmit beamforming [5], [6] requires near perfect CSI at the transmitter for computing the beamforming weight in order to achieve beamforming gain.

For the sake of efficiently exploiting the available radio spectrum, joint coding and modulation or Coded Modulation (CM) schemes were first proposed by Ungerböck in 1982 [7] for non-dispersive Gaussian channels. The benefit of TCM is that it is capable of achieving a coding gain in comparison to uncoded transmissions by expanding the modulation phasor constellation and hence absorbing the parity bits without bandwidth expansion, when transmitting over non-dispersive Gaussian channels. Ungerböck's contribution motivated intensive research on the topic, especially after the conception of turbo codes by Berrou *et al.* [8], leading to Turbo TCM (TTCM) invented by Robertson and Wörz [9]. Further advances were made in the context of designing CM schemes for wireless Rayleigh fading channels by Zehavi [10], by Caire, Taricco and Biglieri [11] in the context of Bit-Interleaved Coded Modulation (BICM) as well as by Li and Ritcey [12], leading to the concept of iteratively decoded BICM (BICMID). Hence, we will employ TCM, BICM, TTCM and BICMID schemes for achieving bandwidth efficiency in the eigen beamforming system.

The financial support of the European Union under the auspices of the Newcom and Phoenix projects, as well as that of the EPSRC UK is gratefully acknowledged.

A reliable channel predictor is imperative for aiding a transmit beamforming scheme to achieve its optimal gain. In this contribution, we will employ the Minimum Mean Square Error (MMSE) based pilot-symbol aided MIMO channel predictor [13]–[15]. However, the quality of CSI predicted by practical channel predictor is still falling short of the high requirement of an eigen beamforming due to the phase ambiguity inherent in the estimated eigen-vectors. In order to mitigate the phase-ambiguity problem differential modulation will also be invoked.

## II. System Overview

Consider a transceiver system having $M_T$ transmit antennas and $M_R$ receive antennas communicating over flat Rayleigh fading channel. The received $M_R$-dimensional symbols vector $\mathbf{y}$ can be expressed as

$$\mathbf{y} = \mathbf{H}\mathbf{x} + \mathbf{n} \tag{1}$$

where $\mathbf{x}$ is the $M_T$-dimensional transmitted symbol vector and $\mathbf{H}$ is a $(M_R \times M_T)$-dimensional complex channel matrix, which is given by

$$\mathbf{H} = \begin{bmatrix} h_{11} & h_{12} & \cdots & h_{1M} \\ h_{21} & h_{22} & \cdots & h_{2M} \\ \vdots & \vdots & \ddots & \vdots \\ h_{M_R1} & h_{M_R2} & \cdots & h_{M_RM_T} \end{bmatrix} \tag{2}$$

where $h_{ij}$ is the channel coefficient between the $i$th receive and $j$th transmit antennas. Furthermore, in (1) $\mathbf{n}$ is the $M_R$-dimensional AWGN vector having a zero-mean and a variance of $E(\mathbf{n}\mathbf{n}^H) = \sigma_n^2 \mathbf{I}_{M_R}$. With the aid of the Singular Value Decomposition (SVD) [16] the $M_r \times M_t$-dimensional channel matrix $\mathbf{H}$ may be decomposed as:

$$\mathbf{H} = \mathbf{U}\mathbf{D}\mathbf{V}^H , \tag{3}$$

where $\mathbf{D}$ is an $M_r \times M_t$ non-negative and diagonal matrix, while $\mathbf{U}$ and $\mathbf{V}$ are $M_r \times M_r$ and $M_t \times M_t$ unitary matrices, respectively. Furthermore, the diagonal entries of $\mathbf{D}$ are the non-negative square roots of the eigenvalues of the matrix $\mathbf{H}\mathbf{H}^H$.

Figure 1 shows the simplified block diagram of differential CM assisted eigen beamforming system. A sequence of information symbols $\{u_k\}$, where the subscript $k$ denotes the time index, are first CM-encoded to yield $\{x'_k\}$ before entering the differential encoder where the sequence $\{v_k\}$ is produced. At the transmit beamforming block, $v_k$ is multiplied by the beamforming weight vector $\mathbf{v}_{(1)k}$ to produce $\mathbf{x}_k$, where $\mathbf{v}_{(1)k}$

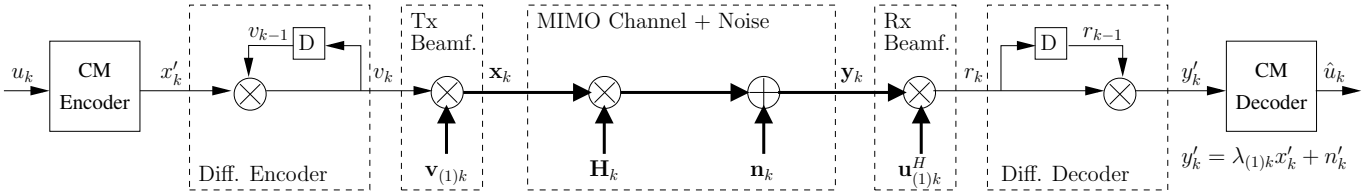


Fig. 1. The simplified block diagram of differential CM assisted eigen beamforming system.

is the first column vector of the unitary matrix $\mathbf{V}$ computed using SVD in (3). At the receiver, receive beamforming is carried out with the aid of a beamforming weight vector of $\mathbf{u}^H_{(1)k}$, which is the conjugate transpose of the first column vector of the unitary matrix $\mathbf{U}$ in (3). Then differential decoding is carried out followed by CM decoding. By ignoring the time index $k$, the signal before the differential decoder can be simplified as:

$$\begin{aligned} r &= \mathbf{u}^H_{(1)} y \ , \\ &= \mathbf{u}^H_{(1)} \mathbf{H} \mathbf{v}_{(1)} v + \mathbf{u}^H_{(1)k} n \ , \\ &= \sqrt{\lambda_{(1)}} v + \breve{n} \ , \end{aligned} \tag{4}$$

where we have $\mathbf{u}^H_{(1)} \mathbf{H} \mathbf{v}_{(1)} = \mathbf{u}^H_{(1)} \mathbf{U} \mathbf{D} \mathbf{V}^H \mathbf{v}_{(1)} = \sqrt{\lambda_{(1)}}$ and $\breve{n} = \mathbf{u}^H_{(1)k} n$. Note that $\sqrt{\lambda_{(1)}}$ is the first diagonal value of the matrix $\mathbf{D}$ in (3), where $\lambda_{(1)}$ is the first eigen value of the matrix $\mathbf{H}\mathbf{H}^H$. Hence, the transmit and receive beamforming has converted a MIMO channel into a Single-Input Single-Output (SISO) channel having a single channel coefficient given by $\sqrt{\lambda_{(1)}}$. The variance of the Additive White Gaussian Noise (AWGN) $\breve{n}$ is the same as that of the original AWGN $n$, which is given by $N_0$.

Note however that, when the predicted channel $\tilde{\mathbf{H}}$ is not perfect, the signal subspace defined by the unitary matrices $\mathbf{U}$ and $\mathbf{V}$ of (3) is not unique [17]. This is because the singular vector/matrix can be different up to a complex-valued coefficient of unit norm [18]. Hence it may cause phase ambiguity [18]. One way to resolve this problem is by employing differential coding [18]. The schematic of differential encoder is shown in Figure 1 between the CM encoder and the transmit beamformer. As seen in Figure 1, the symbol $v_k$ transmitted at time instant $k$ is obtained from:

$$v_k = x'_k v_{k-1} \ , \tag{5}$$

where $x'_k$ is a CM encoded symbol and $v_{k-1}$ is the symbol transmitted at time instant $(k-1)$ [16]. Let us employ PSK-based CM schemes, where we have $|x'_k|^2 = |v_k|^2 = 1$, and assume that the channel coefficient $\sqrt{\lambda_{(1)}}$ in (4) is constant across during the time instant $k$ and $(k-1)$. With the aid of (5) and by introducing the time index $k$ to (4), we have:

$$\begin{aligned} y'_k &= r_k r_{k-1} \ , \\ &= \lambda_{(1)k} v_k v_{k-1} + \sqrt{\lambda_{(1)k}} v_k \breve{n}_{k-1} + \\ &\quad \sqrt{\lambda_{(1)k-1}} v_{k-1} \breve{n}_k + \breve{n}_k \breve{n}_{k-1} \ , \\ y'_k &= \lambda_{(1)k} x'_k + n'_k \ . \end{aligned} \tag{6}$$

Hence, an additional differential encoding and decoding pair in an eigen beamforming scheme is another SISO channel having a channel coefficient of $\lambda_{(1)k}$ and an AWGN of $n'_k = \sqrt{\lambda_{(1)k}} v_k \breve{n}_{k-1} + \sqrt{\lambda_{(1)k-1}} v_{k-1} \breve{n}_k + \breve{n}_k \breve{n}_{k-1}$. The variance of the AWGN $n'_k$ can be computed as $2\lambda_{(1)k} N_0$, where again $N_0$ is the variance of the original AWGN in the channel. As a result, the logarithmic-domain channel soft metric can be computed at the CM decoder as:

$$Pr(y'_k | x'_k = x'^{(m)}) = -\frac{\left| y'_k - \lambda_{(1)k} x'^{(m)} \right|^2}{2\lambda_{(1)k} N_0} \ , \tag{7}$$

where $x'^{(m)}$, for $m \in \{0, 1, \ldots, M-1\}$, is the $m$th phasor in an $M$-ary PSK modulation.

## III. MIMO Channel Prediction

The block diagram of the channel prediction aided differential CM assisted eigen beamforming system is shown in Figure 2, where $\tilde{(.)}$ denotes the predicted value of $(.)$. Transmit and receive buffers are used so that a CM-encoded frame may be partitioned into shorter subframes, where each subframe is added $M_t$ number of pilot symbols at its beginning. A shorter subframe symbol length would increase the accuracy of the channel predictor but would require a higher pilot symbol overhead. During the transmission of the pilot symbols, only one transmit antenna is activated during a symbol period while other transmit antennas are kept silent [13], [14] as seen in Figure 3.

Let us denote the index of the subframe using the subscript $l$ and denote 'subframe' as 'frame' for brevity in this section. For the $l$th frame at time instant $m_t$ $(1 \leq m_t \leq M_T)$, the received signal $y_{m_r}(l, m_t)$ by the $m_r$th $(1 \leq m_r \leq M_R)$ receiver antenna is given by:

$$y_{m_r}(l, m_t) = h_{m_r m_t}(l, m_t) x_p + n_{m_r}(l, m_t) \ , \tag{8}$$

where $h_{m_r m_t}(l, m_t)$ represents the channel coefficient between the $m_t$th transmit antenna and $m_r$th receive antenna for the $l$th frame at time instant $m_t$ while $x_p$ represents the pilot symbol which is assumed to be the same for all transmit antennas for all frames. Furthermore, $n_{m_r}(l, m_t)$ is the AWGN at the $m_r$th receiver antenna for the $l$th frame at time instant $m_t$.

With the aid of the $M_t$-by-$M_t$ pilot symbol matrix as seen in Figure 3, a MIMO channel prediction problem is decomposed into a SISO channel prediction case, such that any SISO prediction algorithm can be applied directly. In this contribution, MMSE based narrowband channel prediction is invoked. Specifically, we construct the following $p$-dimensional vector:

$$\mathbf{y}_{m_r}(l, m_t) = [y_{m_r}(l - p + 1, m_t) \ \cdots \ y_{m_r}(l, m_t)]^T \ , \tag{9}$$

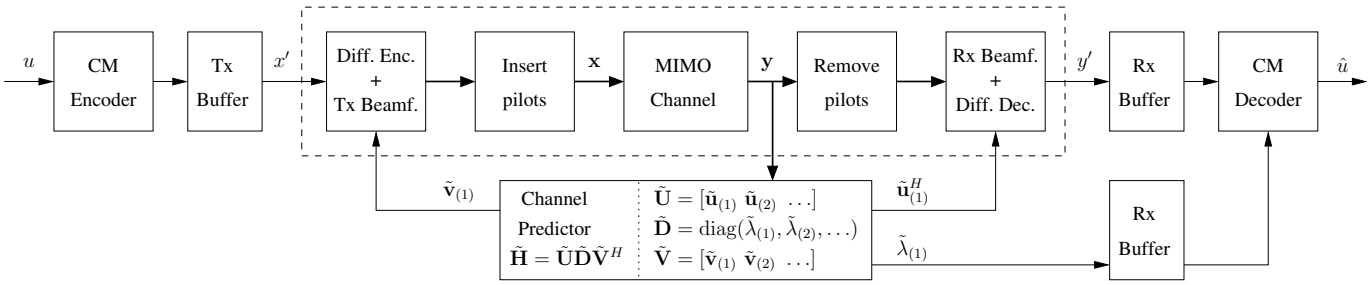


Fig. 2. The block diagram of the channel prediction aided differential CM assisted eigen beamforming system.

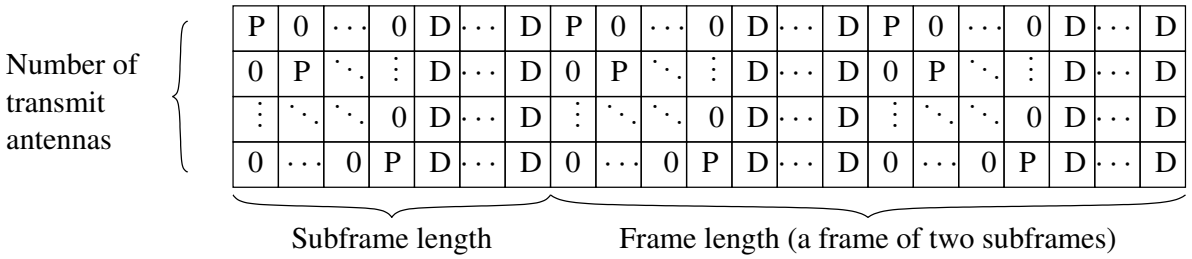


Fig. 3. Schematic of MIMO transmission. The notations $P$, $D$ and 0 denote pilot symbol, data symbol and zero-energy symbol, respectively.

then the predicted channel coefficient $\hat{y}_{m_r}(l+1, m_t)$ of $y_{m_r}(l+1, m_t)$ corresponding to the position of a pilot symbol is given by [15]:

$$\hat{y}_{m_r}(l+1, m_t) \quad = \quad \mathbf{d}_0 \mathbf{y}_{m_r}(l, m_t) \ , \tag{10}$$

where $\mathbf{d}_0$ is given by:

$$\mathbf{d}_0 = \mathbf{R}^{-1}_{\mathbf{y}_{m_r}(l,m_t)} \mathbf{r}_{\mathbf{y}_{m_r}(l,m_t) y_{m_r}(l+1,m_t)} \ , \tag{11}$$

where $\mathbf{R}_{\mathbf{y}_{m_r}(l,m_t)}$ is a $(p \times p)$-dimensional autocorrelation matrix of $\mathbf{y}_{m_r}(l, m_t)$, which is given by [15]:

$$\mathbf{R}_{\mathbf{y}_{m_r}(l,m_t)} = E[\mathbf{y}_{m_r}(l, m_t) \mathbf{y}^H_{m_r}(l, m_t)] \ . \tag{12}$$

Furthermore, $\mathbf{r}_{\mathbf{y}_{m_r}(l,m_t) y_{m_r}(l+1,m_t)}$ is a $p$-dimensional cross-correlation vector between $\mathbf{y}_{m_r}(l, m_t)$ and $y_{m_r}(l+1, m_t)$, which is given by [15]:

$$\mathbf{r}_{\mathbf{y}_{m_r}(l,m_t) y_{m_r}(l+1,m_t)} = E[\mathbf{y}^*_{m_r}(l, m_t) y_{m_r}(l+1, m_t)] \ . \tag{13}$$

Finally, the predicted channel coefficients corresponding to the data symbol can be obtained with the aid of linear interpolation [19].

## IV. Simulation Results

Let us consider a communication over correlated Rayleigh fading channels having a normalised Doppler frequency of $10^{-3}$ and a subframe length of $L_s = 100$ data symbols as well as a frame length of $L_f = 1000$ data symbols when employing CM or Differential-coded CM (D-CM) schemes. The number of transmit antennas is fixed to $M_t = 2$ and the number of receive antennas is fixed to $M_r = 2$. The block diagram of a non-differential coded CM assisted eigen beamforming system is the same as that in Figure 1 but without the differential encoder and decoder blocks.

For the sake of a fair comparison, the CM schemes employed exhibit a similar decoding complexity in terms of the number of decoding states and the number of decoding iterations. For a TCM or BICM code of memory $\nu$, the corresponding complexity is proportional to the number of decoding states $S = 2^\nu$. Since TTCM schemes invoke two component TCM codes, a TTCM code with $t$ iterations and using an $S$-state component code exhibits a complexity proportional to $2.t.S$ or $t.2^{\nu+1}$. As for BICMID schemes, only one decoder is used but the demodulator is invoked in each decoding iteration. However, the complexity of the demodulator is assumed to be insignificant compared to that of the decoder. Hence, a BICMID code with $t$ iterations using an $S$-state code exhibits a complexity proportional to $t.S$ or $t.2^M$. For these reasons, we fix $S = 64$ for TCM and BICM schemes as well as $S = 8$ and $t = 4$ for TTCM schemes, while $S = 8$ and $t = 8$ for BICMID schemes. The code polynomials used for the CM schemes can be found from [20].

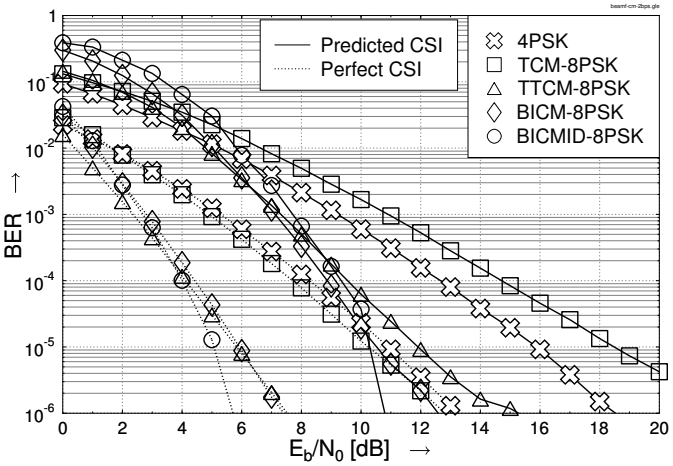


Fig. 4. BER versus $E_b/N_0$ performance of the 4PSK($L_f = L_s = 100$) and CM-8PSK($L_f = 1000, L_s = 100$) beamforming schemes, when communicating over correlated Rayleigh fading channels having a normalised Doppler frequency of $10^{-3}$.

Figure 4 shows the Bit Error Ratio (BER) versus Signal-to-Noise Ratio (SNR) per bit, namely $E_b/N_0$, performance of the 4PSK and CM-8PSK assisted eigen beamforming schemes when employing perfect and predicted CSI without differential coding. As we can see from Figure 4, the performance of the schemes suffer from significant degradation when the CSI is imperfect. For example, at BER=$10^{-5}$ about 8.5 dB and 6.2 dB of performance loss incurred when employing a predicted CSI compare to a perfect CSI for the 4PSK and TTCM-8PSK assisted schemes, respectively. This is due to the phase ambiguity problem discussed in Section II. Furthermore, the TCM-8PSK assisted scheme performs worse than the 4PSK assisted scheme when the CSI is imperfect, at the same throughput of 2 bit/symbol. Interestingly, in the context of the eigen beamforming system, BICMID-8PSK assisted schemes outperformed other CM-8PSK assisted schemes, although when communicating over SISO Rayleigh fading channels without beamforming, BICMID-8PSK is outperformed by TTCM-8PSK scheme [20].

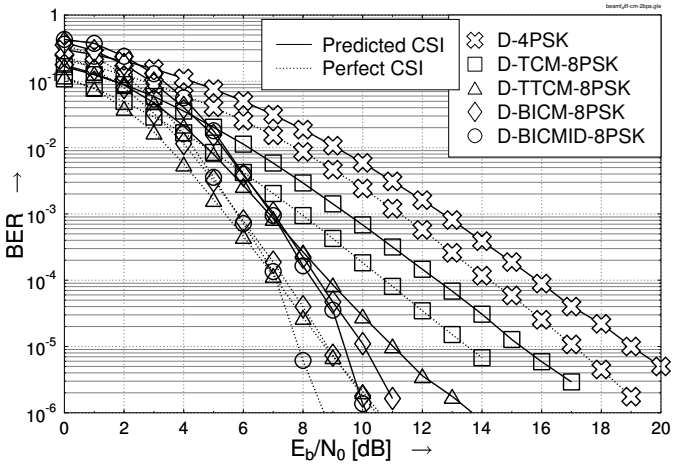


Fig. 5. BER versus $E_b/N_0$ performance of the D-4PSK($L_f = L_s = 100$) and D-CM-8PSK($L_f = 1000, L_s = 100$) beamforming schemes, when communicating over correlated Rayleigh fading channels having a normalised Doppler frequency of $10^{-3}$.

Figure 5 shows the performance of the D-4PSK and D-CM-8PSK assisted eigen beamforming schemes when employing perfect and predicted CSI. As we can see from Figure 5, the performance loss due to employing an imperfect CSI is only about 2 dB for all cases at BER=$10^{-5}$. This is because the differential coding is effective in circumventing the phase ambiguity problem. However, the employment of differential coding comes with a price because it increases the noise variance from $N_0$ to $2\lambda_{(1)k}N_0$ as discussed in Section II. As a result, when the CSI is perfect, the performance of the D-CM-8PSK schemes in Figure 4 is about 3 dB inferior to that of the CM-8PSK schemes in Figure 5. However, as we can see from Figure 6, when the CSI is imperfect, the D-CM-8PSK schemes performs better than the CM-8PSK schemes despite having a higher noise variance. For example, the D-BICMID-8PSK and D-TCM-8PSK schemes perform about 1 dB and 3 dB better than their non-differential coded counterparts at BER=$10^{-5}$. Furthermore, the performance of the uncoded D-4PSK scheme could not outperform the uncoded 4PSK scheme as evidenced in Figure 5 when the CSI is imperfect. This shows the importance of CM schemes in a practical eigen beamforming system. More specifically, the D-BICMID-8PSK scheme yields a coding gain of about 6.5 dB over the 4PSK scheme at a BER of $10^{-5}$. Note that the CM schemes employed were originally designed for employment of non-differential modulation, yet a simple concatenation with differential coding could still yield some performance gains in the context of predicted CSI. Hence, a proper design of differential modulation based CM schemes would yield a higher coding gain.

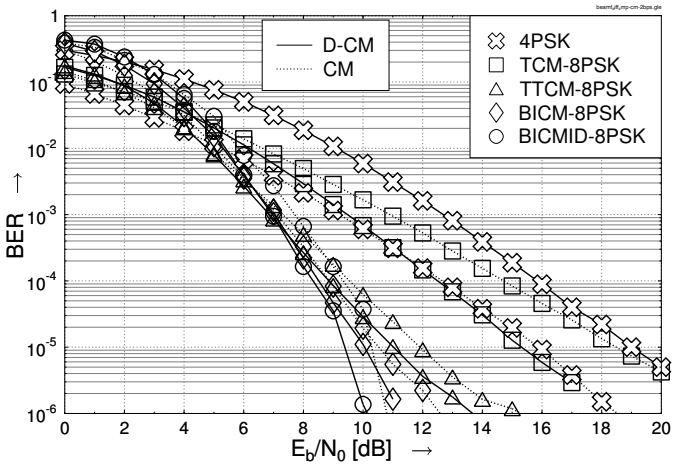


Fig. 6. BER versus $E_b/N_0$ performance of the 4PSK($L_f = L_s = 100$) and CM-8PSK($L_f = 1000, L_s = 100$) beamforming schemes with and without differential coding, when communicating over correlated Rayleigh fading channels having a normalised Doppler frequency of $10^{-3}$ with the aid of an MMSE channel predictor.

Let us now study the effect of channel fading rates in the context of Figures 7 and 8, where the normalised Doppler frequencies of the channels are $10^{-3}$ and $10^{-4}$, respectively. As we can see from Figures 7 and 8, when the normalised Doppler frequencies of the channels is reduced by a factor of 10, it is possible to increase the subframe/frame length by a factor of 10, while maintaining a similar performance.

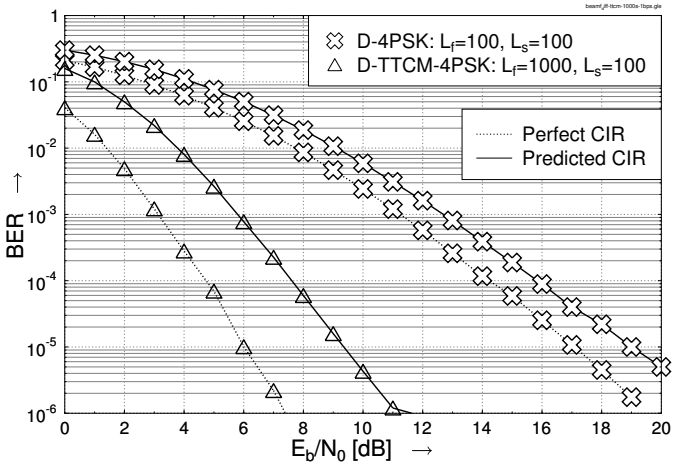


Fig. 7. BER versus $E_b/N_0$ performance of the D-4PSK and D-TTCM-4PSK Beamforming schemes, when communicating over correlated Rayleigh fading channels having a normalised Doppler frequency of $10^{-3}$.

Next, let us study the effect of varying the subframe length at a given frame length of $L_f = 10000$ of the D-CM-4PSK assisted eigen beamforming system in Figure 9. As we can see

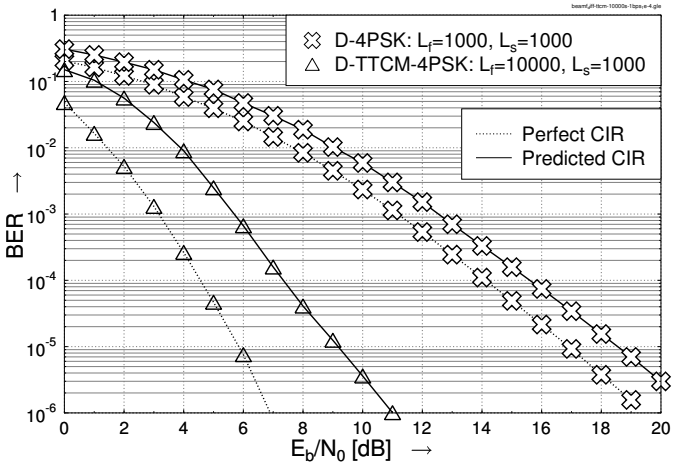


Fig. 8. BER versus $E_b/N_0$ performance of the D-4PSK and D-TTCM-4PSK Beamforming schemes, when communicating over correlated Rayleigh fading channels having a normalised Doppler frequency of $10^{-4}$.

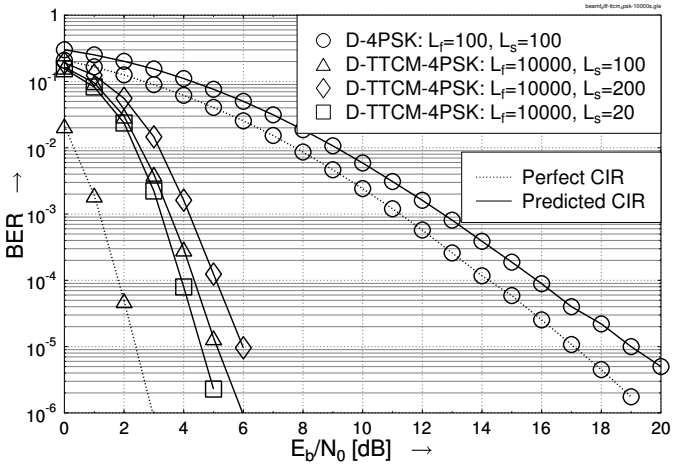


Fig. 9. BER versus $E_b/N_0$ performance of the D-4PSK and D-TTCM-4PSK Beamforming schemes, when communicating over correlated Rayleigh fading channels having a normalised Doppler frequency of $10^{-3}$.

from Figure 9, as the subframe length reduces the accuracy of the channel predictor improves, which resulted in a better performance at the cost of a higher pilot symbol overhead. As an example, there are $L_f/L_s = 500$ subframes of length $L_s = 20$ data symbols in a $L_f = 10000$ data symbol frame, resulting in a pilot symbol overhead of $(M_t L_f/L_s)/(L_f + M_t L_f/L_s) = 1000/11000$, which is about 9%. By contrast, when $L_f$ is fixed to 10000, the pilot symbol overheads for having $L_s = 200$ and $L_s = 100$ are about 1% and 2%, respectively. From Figure 9, using $L_s = 100$ is a good compromise in terms of performance versus pilot symbol overhead.

## V. Conclusions

In this contribution, we have studied a channel prediction aided coded modulation assisted eigen beamforming scheme when communicating over correlated Rayleigh fading channels. It was shown in Figure 6 that both differential coding and coded modulation are needed for assisting an eigen beamforming system when employing a practical channel predictor. A new coded modulation design using differential modulation would further improve the performance of an eigen beamforming system when using a predicted channel state information.

## References


[1] G. Foschini Jr. and M. Gans, "On limits of wireless communication in a fading environment when using multiple antennas," *Wireless Personal Communications*, vol. 6, pp. 311–335, March 1998.

[2] E. Telatar, "Capacity of multi-antenna Gaussian channels," *European Transactions on Telecommunication*, vol. 10, pp. 585–595, Nov–Dec 1999.

[3] V. Tarokh, N. Seshadri and A. R. Calderbank, "Space-time codes for high rate wireless communication: Performance analysis and code construction," *IEEE Transactions on Information Theory*, vol. 44, pp. 744–765, March 1998.

[4] S. M. Alamouti, "A Simple Transmitter Diversity Scheme for Wireless Communications," *IEEE Journal on Selected Areas in Communications*, vol. 16, pp. 1451–1458, October 1998.

[5] F. Rashid-Farrokhi, K. Liu, and L. Tassiulas, "Transmit beamforming and power control for cellular wireless systems," *IEEE Journal on Selected Areas in Communications*, vol. 16, pp. 1437–1450, October 1998.

[6] A. Abdel-Samad, T. N. Davidson and A. B. Gershman, "Robust transmit eigen beamforming based on imperfect channel state information," *IEEE Transactions on Signal Processing*, vol. 54, pp. 1596–1609, May 2006.

[7] G. Ungerböck, "Channel coding with multilevel/phase signals," *IEEE Transactions on Information Theory*, vol. 28, pp. 55–67, January 1982.

[8] C. Berrou, A. Glavieux and P. Thitimajshima, "Near Shannon Limit Error-Correcting Coding and Decoding : Turbo Codes," in *Proceedings, IEEE International Conference on Communications*, pp. 1064–1070, 1993.

[9] P. Robertson, T. Wörz, "Bandwidth-efficient Turbo Trellis-coded Modulation Using Punctured Component Codes," *IEEE Journal on Selected Areas in Communications*, vol. 16, pp. 206–218, February 1998.

[10] E. Zehavi, "8-PSK trellis codes for a Rayleigh fading channel," *IEEE Transactions on Communications*, vol. 40, pp. 873–883, May 1992.

[11] G. Caire, G. Taricco and E. Biglieri, "Bit-Interleaved Coded Modulation," *IEEE Transactions on Information Theory*, vol. IT-44, pp. 927–946, May 1998.

[12] X. Li, J. A. Ritcey, "Trellis-Coded Modulation with Bit Interleaving and Iterative Decoding," *IEEE Journal on Selected Areas in Communications*, vol. 17, pp. 715–724, April 1999.

[13] Z. Luo, H. Gao, Y. Liu, and J. Gao, "Robust pilot-symbol-aided MIMO channel estimation and prediction," in *IEEE Global Telecommunications Conference*, (Dallas, Texas, USA), pp. 3646 – 3650, 29 November - 3 December 2004.

[14] D. V. Duong, B. Holter, and G. E. Oien, "Optimal pilot spacing and power in rate-adaptive MIMO diversity systems with imperfect transmitter CSI," in *IEEE 6th Workshop on Signal Processing Advances in Wireless Communications*, (New York, USA), pp. 47 – 51, 5 - 8 June 2005.

[15] A. Duel-Hallen, S. Hu, and H. Hallen, "Long range prediction of fading signals: enabling adaptive transmission for mobile radio channels," *IEEE Signal Processing Magzine*, vol. 17, pp. 62–75, May 2000.

[16] B. Vucetic and J. Yuan, *Space-Time Coding*. New York: John Wiley-IEEE Press, May 2003.

[17] H. T. Nguyen, G. Leus, and N. Khaled, "Prediction of the eigenvectors for spatial multiplexing MIMO systems in time-varying channels," in *Proceedings of the Fifth IEEE International Symposium on Signal Processing and Information Technology*, (Athens, Greece), pp. 119– 124, 18 - 21 December 2005.

[18] T. Dahl, N. Christophersen, and D. Gesbert, "Blind MIMO eigenmode transmission based on the algebraic power method," *IEEE Transactions on Signal Processing*, vol. 52, pp. 2424– 2431, September 2004.

[19] S. Coleri, M. Ergen, A. Puri, and A. Bahai, "Channel estimation techniques based on pilot arrangement in OFDM systems," *IEEE Transactions on Broadcasting*, vol. 48, pp. 223 – 229, September 2002.

[20] L. Hanzo, S. X. Ng, W. Webb and T.Keller, *Quadrature Amplitude Modulation: From Basics to Adaptive Trellis-Coded, Turbo-Equalised and Space-Time Coded OFDM, CDMA and MC-CDMA Systems, Second Edition*. New York, USA : John Wiley and Sons, 2004.